

# The ion-atom absorption processes as one of the factors of the influence on the sunspot opacity

Lj. M. Ignjatović,<sup>1,2</sup> A. A. Mihajlov,<sup>1,2</sup> V. A. Srećković<sup>1,2</sup> and M. S. Dimitrijević<sup>2,3,4,5</sup>

<sup>1</sup> *University of Belgrade, Institute of Physics, P. O. Box 57, 11001 Belgrade, Serbia*

<sup>2</sup> *Isaac Newton Institute of Chile, Yugoslavia Branch, Volgina 7, 11060 Belgrade, Serbia*

<sup>3</sup> *Astronomical Observatory, Volgina 7, 11160 Belgrade 74, Serbia*

<sup>4</sup> *IHIS-Technoexperts, Bežanijska 23, 11080 Zemun, Serbia*

<sup>5</sup> *Observatoire de Paris, 92195 Meudon Cedex, France*

## ABSTRACT

As a continuation of the previous investigations of the symmetric and strongly non-symmetric ion-atom absorption processes in the far UV region within the models of the quiet Sun photosphere, these processes are studied here within a model of the sunspot. Here we mean the absorption processes in the  $\text{H}(1s)+\text{H}^+$  and  $\text{H}(1s)+X^+$  collisions and the processes of the photo-dissociation of the  $\text{H}_2^+$  and  $\text{HX}^+$  molecular ions, where  $X$  is one of the metal atoms:  $X=\text{Na}, \text{Ca}, \text{Mg}, \text{Si}$  and  $\text{Al}$ . Obtained results show that the influence of the considered ion-atom absorption processes on the opacity of sunspots in the considered spectral region ( $110\text{ nm} \lesssim \lambda \lesssim 230\text{ nm}$ ) is not less and in some parts even larger than the influence of the referent electron-atom processes. In such a way, it is shown that the considered ion-atom absorption processes should be included *ab initio* in the corresponding models of sunspots of solar-type and near solar-type stars. Apart of that, the spectral characteristics of the considered non-symmetric ion-atom absorption processes (including here the case  $X=\text{Li}$ ), which can be used in some further applications, have been determined and presented within this work.

**Key words:** stars: atmospheres – sunspots: general – radiative transfer – atomic processes – molecular processes

## 1 INTRODUCTION

In the previous investigations the significant influence of the relevant ion-atom absorption processes on the solar photosphere opacity was already demonstrated. So, in Mihajlov & Dimitrijević (1986); Mihajlov et al. (1993, 1994) and Mihajlov et al. (2007)) have been studied such symmetric ion-atom processes, as the molecular ion  $\text{H}_2^+$  photo-dissociation

$$\varepsilon_\lambda + \text{H}_2^+ \longrightarrow \text{H} + \text{H}^+, \quad (1)$$

and the absorption charge exchange in  $(\text{H}^+ + \text{H})$ -collisions

$$\varepsilon_\lambda + \text{H}^+ + \text{H} \longrightarrow \text{H} + \text{H}^+, \quad (2)$$

where  $\text{H}=\text{H}(1s)$ ,  $\text{H}_2^+$  is the hydrogen molecular ion in the ground electronic state, and  $\varepsilon_\lambda$  - the energy of a photon with the wavelength  $\lambda$ . The significance of these processes was established within the solar photosphere models from Vernazza et al. (1981) and Maltby et al. (1986) in the optical, and from Vernazza et al. (1981) in far UV and EUV regions of  $\lambda$ . Later, the symmetric processes (1) - (2) were in-

cluded *ab initio* in one of the new solar photosphere models (Fontenla et al. 2009).

Then, in Mihajlov et al. (2013) was undertaken the investigation of some non-symmetric ion-atom absorption processes, namely the photo-dissociation and photo-association of the the molecular ions

$$\varepsilon_\lambda + \text{HX}^+ \longrightarrow \text{H}^+ + X, \quad (3)$$

$$\varepsilon_\lambda + \text{H} + X^+ \longrightarrow (\text{XH}^+)^*, \quad (4)$$

and the absorption charge-exchange in the ion-atom collisions

$$\varepsilon_\lambda + \text{H} + X^+ \longrightarrow \text{H}^+ + X, \quad (5)$$

where  $X$  is the ground state atom of one of metals, relevant for the used solar photosphere model, whose ionization potential  $I_X$  is smaller than the hydrogen atom ionization potential  $I_{\text{H}}$ ,  $X^+$  - the corresponding atomic ion in its ground state,  $\text{HX}^+$  and  $(\text{XH}^+)^*$  - the molecular ion in the electronic states which are adiabatically correlated (at the infinite internuclear distance) with the states of the ion-atom systems

$H + X^+$  and  $H^+ + X$  respectively. These processes were examined within the same solar photosphere model as in Mihajlov et al. (2007), i.e. the model C from Vernazza et al. (1981), with  $X = \text{Mg, Si and Al}$ . Also, in accordance with the composition of the solar atmosphere, the processes of the type (3) - (5), but with atom  $\text{He}(1s^2)$  and ion  $H^+$  instead  $H$  and  $X^+$ , were included in the consideration. However, it was established that in the case of this atmosphere (for the difference of some helium reach stellar atmospheres considered in Ignjatović et al. (2014)) such processes can be practically neglected. Since the ion-atom systems with the mentioned  $X$  are strongly non-symmetric, the examined processes generate the quasi-molecular absorption bands in the neighborhoods of  $\lambda$  which correspond to the energies  $\Delta_{H,X} \equiv I_H - I_X$ . According to the values of  $\Delta_{H,X}$  with the mentioned  $X$  these absorption bands lie in the part of the far UV region. We should note here that the photo-dissociation of the molecular ion  $\text{HSi}^+$  was considered first time from the astrophysical aspect (interstellar clouds and the atmospheres of red giant stars) in Stancil et al. (1997).

In Mihajlov et al. (2013) was shown that, in the case of the quiet Sun, ion-atom processes (1) - (2) and (3) - (5) together become seriously concurrent to some other relevant absorption processes in far UV and EUV regions within the whole solar photosphere. This result is especially important, since among all possible ion-atom non-symmetric processes only those of them, for which the needed data about the corresponding molecular ions were known, were taken into account. Because of that, it was natural to conclude that the non-symmetric processes (3) - (5) should be also included *ab initio* in the corresponding solar photosphere models.

One can see that the previous investigations of the ion-atom absorption processes were performed only in the case of the quiet Sun. However, it is well known how significant role for the solar atmosphere the sunspots play, and certainly it was interesting to see what is the situation with these processes in such objects. Because of that, this investigation, whose some preliminary results were referred recently on a corresponding astrophysical conference Srećković et al. (2013), was undertaken. All considerations were within the sunspot model M from Maltby et al. (1986). Such choice was caused by the fact that only this model, among other models mentioned in the literature (see e.g. Fontenla et al. (2006)), provided all data needed for the calculations of the absorption coefficients which characterize the considered absorption processes. Certainly, the ion-atom absorption processes of the type (3) - (5) were included in the considerations. However, here we take into account also additional processes of the molecular ion photo-dissociation and photo-association

$$\varepsilon_\lambda + \text{HX}^+ \longrightarrow \text{H} + \text{X}^{++}, \quad (6)$$

$$\varepsilon_\lambda + \text{H} + \text{X}^+ \longrightarrow \text{HX}^{++}, \quad (7)$$

where  $\text{X}^{++}$  is the ion in excited state with the excitation energy  $E_{exc}(\text{X}^{++}) \lesssim \Delta_{H,X}$  and  $\text{HX}^{++}$  - the molecular ion in the electronic state adiabatically correlated with the state of the  $\text{H} + \text{X}^{++}$  system, as well as the corresponding collisional excitation

$$\varepsilon_\lambda + \text{H} + \text{X}^+ \longrightarrow \text{H} + \text{X}^{++}, \quad (8)$$

which realizes over creation of the quasimolecular complex  $(\text{H} + \text{X}^+)^*$  in the excited electronic state adiabatically correlated with the state of the same system  $\text{H} + \text{X}^{++}$  as in the process (7). Depending of the values of  $E_{exc}(\text{X}^{++})$  the absorption bands generated by the processes (6) - (8) can lie not only in far UV region of  $\lambda$ , but also in near UV and visible regions. The reason for the consideration of these processes is the fact that the absorption bands generated by some of them overlap with the bands generated by the processes (1) - (2) and (3) - (5). If the radiative transition  $\text{X}^+ \rightarrow \text{X}^{++}$  is allowed by the dipole selection rules the corresponding absorption band can be treated, as in the case of the similar phenomena caused by atom-atom collisions (Veža et al. (1998); Skenderović et al. (2002)), i.e. as the satellite of the ion spectral line connected with the mentioned transition.

The basic task of this investigation is to estimate the significance of the symmetric and non-symmetric ion-atom absorption processes in the case of the sunspot with respect to the processes of the negative hydrogen ion  $\text{H}^-$  photo-detachment and inverse "bremsstrahlung" in  $(e + \text{H})$ -collisions, namely

$$\varepsilon_\lambda + \text{H}^- \longrightarrow \text{H} + e', \quad (9)$$

$$\varepsilon_\lambda + e + \text{H} \longrightarrow \text{H} + e', \quad (10)$$

where  $e$  and  $e'$  denote the free electron in initial and final channel, which, similarly to the previous papers, are treated here as the referent processes. It is connected with the concept of this paper which stays the same as in all previous papers. Namely, the aim of these papers (see e.g. Mihajlov et al. (1993, 2007, 2013)) was to pay attention on the considered ion-atom radiative processes as the factors of the influence on the opacity of the solar atmosphere. For that purpose it was needed (and enough in the same time) to show that the efficiency of these processes in the considered spectral region is close to the efficiency of some known radiative processes whose significance for the solar atmosphere is accepted in literature. It is clear that in the case of this atmosphere just the electron-atom processes (9) and (10) can be taken as the referent ones. Because of that in these previous papers many other radiative processes have not been considered, including here the certainly very important processes of the metal atom photo-ionization, which were already discussed in the literature in connection with the quiet Sun atmosphere in Fontenla et al. (2011). We mean the processes

$$\varepsilon_\lambda + (\text{X})_g^* \longrightarrow \text{X}^+ + e', \quad (11)$$

where  $(\text{X})_g^*$  denotes the given metal atom in the ground state, i.e.  $\text{X}_g$ , or in any possible (under the considered conditions) excited state, i.e.  $\text{X}^*$ . However, within the sunspot we have a significantly smaller temperature than in the quiet Sun photosphere (see figure about model) and consequently it is possible to expect there more larger efficiency of these photo-ionization processes, so that the position of the mentioned electron-atom processes as the referent ones is not so clear. Because of that the processes of the metal atom photo-ionization were taken into account from the beginning of this investigation (some of them were considered already in Srećković et al. (2013)). In accordance with above mentioned the following absorption processes are included in the consideration in this work:

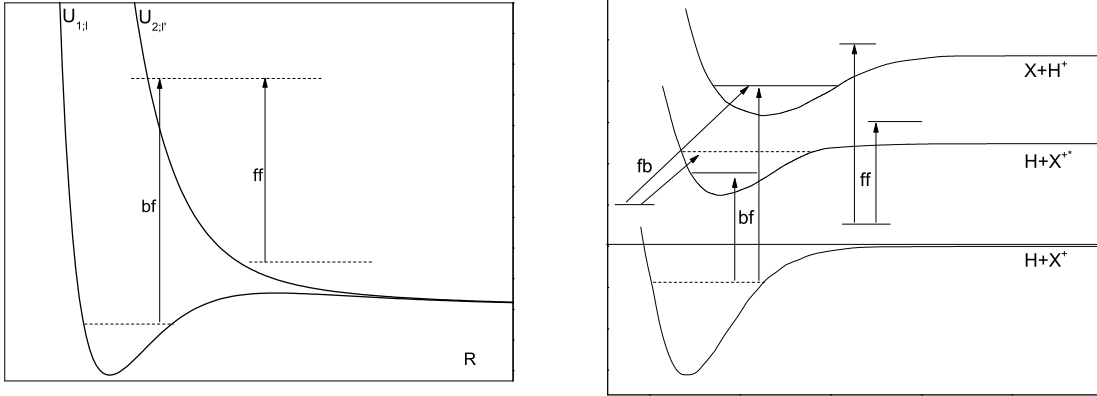


**Figure 1.** *Left panel a:* The bound-free (bf) and free-free (ff) transitions in the case of the symmetric ion-atom processes (1) - (2). *Right panel b:* The bound-free (bf), free-free (ff) and free-bound (fb) transitions in the case of the non-symmetric ion-atom processes:  $\longrightarrow$  - Eqs. (3) - (5),  $\dashrightarrow$  - Eqs. (6) - (8).

- the symmetric ion-atom processes (1) - (2);
- the non-symmetric processes (3) - (5) with  $X = \text{Na, Ca, Mg, Si and Al}$ , for which the needed data about the corresponding molecular ions  $\text{HX}^+$  are known;
- the non-symmetric processes (6) - (8) with  $X^{++} = \text{Ca}^+(3p^63d), \text{Ca}^+(3p^64p), \text{Ca}^+(3p^65s), \text{Ca}^+(3p^64d), \text{Ca}^+(3p^65p)$  and  $\text{Al}^+(2p^63s3p)$ ,
- the electron-atom processes (9) and (10);
- the photo-ionization processes (11) with all metal atoms relevant for the used sunspots model, i.e. including the case  $X = \text{Fe}$ .

Let us note that as in Srećković et al. (2013) only such non-symmetric processes are taken into account here for which all needed data about the corresponding molecular ions are known from the literature.

It is well known that inside sunspot is needed to take into account the presence of its magnetic field. In connection with this we have to note that according to the existing data (see e.g. Penn & Livingston (2011)) this field is always not larger than 4000 Gs. This is very important for us since it can be shown that in our further considerations the presence of such magnetic field can be completely neglected and all needed calculations can be performed as in the case of the quiet Sun.

The aims of this work request determination of the corresponding spectral absorption coefficients for all mentioned ion-atom processes, as well as for the concurrent absorption processes (9) - (10) and (11), as functions of  $\lambda$  and the height  $h$  above the referent solar atmosphere layer. In this context the processes (1) - (2), (3) - (5) and (6) - (8) are treated as the processes from the groups "1", "2" and "3" respectively, which is denoted by the corresponding index:  $j = 1, 2$  or  $3$ . Let us note that here the spectral characteristics of the non-symmetric processes of the type (3) - (4), but with  $X = \text{Li}$ , are also determined in rather wide regions of the temperatures and wavelengths. Namely, such processes could be of interest for lithium rich stellar atmospheres ("Li stars", Hack et al. (1997); Shavrina et al. (2001, 2003)) as an additional canal for the creation of the neutral lithium atoms.

All relevant matter is distributed below in five Sections

and two Appendices. So, the expressions of the considered absorption processes are given in the Sections 2 and 3, together with the needed comments about the methods of their determination. The Section 4 contains the needed comments about used calculation methods. The results of the calculations of the spectral coefficients and other quantities, which characterize the relative efficiencies of the considered processes, are presented (with the corresponding discussions) in the Section 4, and in the last Section 5 are given some conclusions and are indicated directions of the further investigations. Then, the potential curves and dipole matrix elements of the molecular ions  $\text{HX}^+$  with  $X = \text{Na}$  and  $\text{Li}$ , which are determined within this work, are given in Appendix A. Finally, some of the spectral characteristics of the processes (3) - (5) and (6) - (8), which can be used in some other applications, are presented in Appendix B.

## 2 THE SPECTRAL CHARACTERISTICS OF THE ION-ATOM ABSORPTION PROCESSES

### 2.1 The partial ion-atom absorption coefficients

The above mentioned ion-atom absorption processes, namely:

- the photo-dissociation (bound-free) processes (1), (3) and (6),
- photo-association (free-bound) processes (4) and (7),
- absorption charge-exchange and collisional excitation (free-free) processes (2), (5) and (8)

are illustrated by Fig. 1. The efficiencies of these processes are characterized in this work by the corresponding partial spectral absorption coefficients denoted with:

- $\kappa_{ia;1}^{(bf)}(\lambda; h)$ ,  $\kappa_{iaX;2}^{(bf)}(\lambda; h)$  and  $\kappa_{iaX;3}^{(bf)}(\lambda; h)$ ,
- $\kappa_{iaX;2}^{(fb)}(\lambda; h)$  and  $\kappa_{iaX;3}^{(fb)}(\lambda; h)$ , -  $\kappa_{ia;1}^{(ff)}(\lambda; h)$ ,  $\kappa_{iaX;2}^{(ff)}(\lambda; h)$  and  $\kappa_{iaX;3}^{(ff)}(\lambda; h)$  respectively.

In accordance with the previous papers these coefficients are given by the similar expressions, namely

$$\kappa_{ia;1}^{(bf,ff)}(\lambda; h) = K_{ia;1}^{(bf,ff)}(\lambda, T) \cdot N_{\text{H}} N_{\text{H}^+}, \quad (12)$$

$$\kappa_{iaX;j}^{(bf,fb)}(\lambda; h) = K_{iaX;j}^{(bf,fb)}(\lambda, T) \cdot N_{\text{H}} N_{X^+}, \quad j = 2, 3, \quad (13)$$

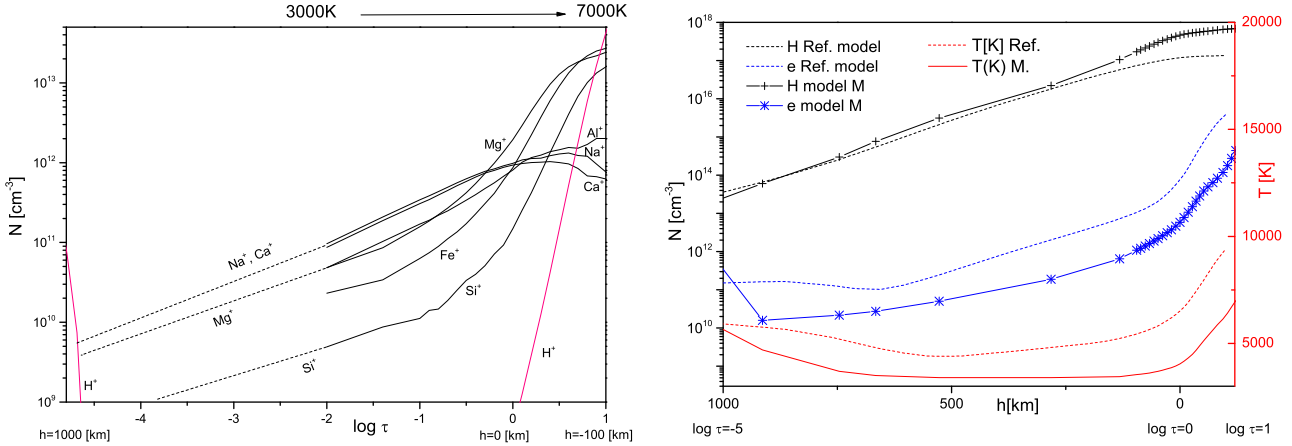


**Figure 2.** Left panel **a**:: The hydrogen and metal ion densities  $N_{H^+}$  and  $N_{X^+}$  for the sunspot umbral model M from Maltby et al. (1986). Right panel **b**:: The local temperature  $T$  and the densities  $N(e)$  and  $N(H)$  of the free electrons and hydrogen atoms for the sunspot model M and referent model of the quiet Sun atmosphere from Maltby et al. (1986).

$$\kappa_{iaX;j}^{(fb)}(\lambda; h) = K_{iaX;j}^{(fb)}(\lambda, T) \cdot N_H N_{X^+}, \quad j = 2, 3, \quad (14)$$

where  $K_{ia;1}^{(bf,ff)}(\lambda, T)$ ,  $K_{iaX;j}^{(bf,ff)}(\lambda, T)$  and  $K_{iaX;j}^{(fb)}(\lambda, T)$ , where  $j = 2$  and  $3$ , are the corresponding rate coefficients. With  $T$ ,  $N_H$ ,  $N_{H^+}$  and  $N_{X^+}$  are denoted here the local temperature and densities of the hydrogen atoms and ions  $H^+$  and  $X^+$  respectively, whose values are taken (for each  $h$ ) from the used sunspot model of Maltby et al. (1986). Here, as in the previous papers, it is understood that the photo-dissociation rate coefficients are defined by the known relations

$$K_{ia;1}^{(bf)}(\lambda, T) = \sigma_{H_2^+}^{(phd)}(\lambda, T) \cdot \chi^{-1}(T; H_2^+), \quad (15)$$

$$K_{iaX;j}^{(bf)}(\lambda, T) = \sigma_{HX^+}^{(phd)}(\lambda, T) \cdot \chi^{-1}(T; HX^+), \quad j = 2, 3, \quad (16)$$

$$\chi(T; H_2^+) = \left[ \frac{N(H)N(H^+)}{N(H_2^+)} \right]_T, \quad (17)$$

$$\chi(T; HX^+) = \left[ \frac{N(H)N(X^+)}{N(HX^+)} \right]_T, \quad (18)$$

where  $\sigma_{H_2^+}^{(phd)}(\lambda, T)$  and  $\sigma_{HX^+}^{(phd)}(\lambda, T)$ , where  $j = 2$  and  $3$ , are the mean thermal photo-dissociation cross-sections: for the molecular ions  $H_2^+$  in the process (1), and for ions  $HX^+$  in the processes (3) and (6) respectively. With  $N_{H_2^+}$  and  $N_{HX^+}$  are denoted the densities of the molecular ions  $H_2^+$  and  $HX^+$ , and the designation  $[...]_T$  denotes that the factors  $\chi(T; H_2^+)$  and  $\chi(T; HX^+)$  are determined under the condition of the local thermodynamical equilibrium (LTE) with given  $T$ .

## 2.2 The total ion-atom absorption coefficients

The total efficiency of the symmetric ion-atom processes (1) - (2), i.e. group "1", is characterized here by the spectral absorption coefficient  $\kappa_{ia;1}(\lambda; h)$ , given by

$$\begin{aligned} \kappa_{ia;1}(\lambda; h) &= K_{ia;1}(\lambda, T) \cdot N(H)N(H^+), \\ K_{ia;1}(\lambda, T) &= K_{ia;1}^{(bf)}(\lambda, T) + K_{ia;1}^{(ff)}(\lambda, T). \end{aligned} \quad (19)$$

In connection with the non-symmetric processes we will introduce firstly the total efficiencies of the processes (3) - (5) and (6) - (8), i.e. groups "2" and "3", for given  $X$  which are characterized by the spectral absorption coefficients  $\kappa_{X;2}(\lambda; h)$  and  $\kappa_{X;3}(\lambda; h)$ . They are given by

$$\kappa_{X;j}(\lambda; h) = K_{X;j}(\lambda, T) \cdot N(H)N(X^+), \quad (20)$$

$$K_{X;j}(\lambda, T) = K_{X;j}^{(bf)}(\lambda, T) + K_{X;j}^{(fb)}(\lambda, T) + K_{X;j}^{(ff)}(\lambda, T), \quad (21)$$

where  $j = 2$  and  $3$ , and  $X$  is the metal atom relevant in these cases. Then, the total efficiencies of the whole groups "2" and "3", i.e. the non-symmetric processes (3) - (5) and (6) - (8) with all relevant  $X$ , are characterized by the spectral absorption coefficients  $\kappa_{ia;2}(\lambda; h)$  and  $\kappa_{ia;3}(\lambda; h)$  given by

$$\kappa_{ia;j}(\lambda; h) = \Sigma_{(X)_j} \kappa_{X;j}(\lambda; h), \quad j = 2, 3, \quad (22)$$

where  $(X)_j$  denotes that the summation is performed over all metal atoms relevant for the processes from the corresponding groups. As the consequence, the efficiency of symmetric and non-symmetric processes (3) - (5) is characterized by the spectral absorption coefficient  $\kappa_{ia;1-2}(\lambda; h)$  given by

$$\kappa_{ia;1-2}(\lambda; h) = \kappa_{ia;1}(\lambda; h) + \kappa_{ia;2}(\lambda; h), \quad (23)$$

and the total efficiency of all considered ion-atom absorption processes - by the corresponding spectral absorption coefficient  $\kappa_{ia}(\lambda; h)$ , namely

$$\kappa_{ia;1-3}(\lambda; h) = \kappa_{ia;1-2}(\lambda; h) + \kappa_{ia;3}(\lambda; h), \quad (24)$$

where the coefficients  $\kappa_{ia;3}(\lambda; T)$  is given by Eq. (22).

## 3 THE SPECTRAL CHARACTERISTICS OF THE CONCURRENT ABSORPTION PROCESSES

The efficiency of the electron-atom absorption processes (9) and (10) are characterized here by the corresponding bound-free (bf) and free-free (ff) spectral absorption coefficients

$\kappa_{ea,bf}(\lambda; h)$  and  $\kappa_{ea,ff}(\lambda; h)$ . They are taken in the usual form

$$\kappa_{ea,bf}(\lambda; h) = K_{ea,bf}(\lambda, T) \cdot N(\text{H})N(e), \quad (25)$$

$$\kappa_{ea,ff}(\lambda; h) = K_{ea,ff}(\lambda, T) \cdot N(\text{H})N(e), \quad (26)$$

from where it follows that the efficiency of these electron-atom processes together is characterized here by the total absorption coefficient  $\kappa_{ea}(\lambda; h)$  given by

$$\begin{aligned} \kappa_{ea}(\lambda; h) &= K_{ea}(\lambda, T) \cdot N(\text{H})N_e, \\ K_{ea}(\lambda, T) &= K_{ea,bf}(\lambda, T) + K_{ea,ff}(\lambda, T). \end{aligned} \quad (27)$$

where  $K_{ea,bf}(\lambda, T)$  and  $K_{ea,ff}(\lambda, T)$  are the corresponding partial rate coefficients. The first of them is defined by the known relations

$$\begin{aligned} K_{ea,bf}(\lambda; h) &= \sigma_{\text{H}^-}^{(phd)}(\lambda) \cdot \chi^{-1}(T; \text{H}^-), \\ \chi(T; \text{H}^-) &= \left[ \frac{N(\text{H})N_e}{N(\text{H}^-)} \right], \end{aligned} \quad (28)$$

where  $\sigma_{\text{H}^-}^{(phd)}(\lambda)$  is the spectral cross-section for the ion  $\text{H}^-$  photo-detachment, the designation  $[\dots]_T$  - is already defined above, and  $N(\text{H})$  and the free electron density  $N(e)$  are taken from the used sunspot model.

Then, the photo-ionization processes (11), which are connected with the metal atoms of the given kinds, are characterized here by the corresponding effective spectral absorption coefficient  $\kappa_{phi;[X]}(\lambda; h)$ , namely

$$\kappa_{phi;X}(\lambda; h) = \sigma_{[X]}^{(phi)}(\lambda; T) \cdot N([X]; h), \quad (29)$$

where  $[X]$  marks the kind of the given metal atoms,  $N([X]; h)$  - the mean local density of all these atoms, i.e. the atoms in the ground state and in all excited states atoms which are realized with existing  $N_e$  and  $T$ , and  $\sigma_{[X]}^{(phi)}(\lambda; T)$  is the corresponding mean (for given  $T$ ) photo-ionization cross-sections.

## 4 THE CALCULATION METHODS

### 4.1 The ion-atom absorption processes

As it is known the spectral rate coefficients introduced in Eqs. (12) - (14) are calculated using the data about the relevant molecular ions characteristics. We mean the potential curves of the initial and final electronic states of the considered molecular ions and the corresponding transition dipole moments. The behavior of these characteristics as the functions of the internuclear distance  $R$  was already shown in the cases of the symmetric and non-symmetric ( $X = \text{Mg}$  and  $\text{Si}$ ) ion-atom processes in Mihajlov et al. (2007) and Mihajlov et al. (2013) respectively. Also, it is illustrated here by figure in the Appendix A in the case  $X = \text{Na}$ . The potential curves and transition dipole moments needed for the non-symmetric processes (3) - (5) with  $X = \text{Na}$  and  $\text{Li}$  are determined within this work and presented in Appendix A. For other above described non-symmetric ion-atom processes they are taken from Mihajlov et al. (2013), Aymar & Dulieu (2012), Nguyen et al. (2011) and Habli et al. (2011), and for symmetric processes - from Mihajlov et al. (2007).

In this work all mentioned ion-atom processes, excluding (2) and (8) with  $X^{++} = \text{Ca}^+(3p^64p)$ , have completely quantum-mechanical treatment, and the corresponding partial rate coefficients are determined in the same way as in Mihajlov et al. (2007) and Mihajlov et al. (2013), where the whole procedure was described in details. Since the transition dipole moment of the system  $\text{H} + \text{H}^+$  unlimitedly increases (with increasing of  $R$ ), the partial rate coefficient for the free-free process (2) is determined here semi-classically, as it was described in Mihajlov et al. (1994) and Mihajlov et al. (2007). Then, in the case of the non-symmetric processes (6) - (8) with  $X^{++} = \text{Ca}^+(3p^64p)$  the radiative transition  $\text{Ca}^+(3p^64s) \rightarrow \text{Ca}^+(3p^64p)$  is allowed by the dipole selection rules and, consequently, quasi-molecular band generated by these processes represent a satellite of the corresponding ion spectral line. In this case the transition dipole moment approaches (when  $R$  increases) to *constant*  $\neq 0$ . Because of that the rate coefficient for this free-free process can be determined by now only semi-classically. However, in this case it is needed to use the semi-classical procedure which is described in Ignjatović et al. (2009) in connection with the ion-atom processes in helium-rich stellar atmospheres. Let us note that the spectral rate coefficients of the considered non-symmetric absorption processes, including the processes with  $X = \text{Li}$ , are presented here in the Appendix B.

### 4.2 The concurrent absorption processes

The electron-atom absorption processes (9) - (10) are described in this work similarly to Mihajlov et al. (1994) and Mihajlov et al. (2007). Because of that the photo-detachment cross-section  $\sigma_{\text{H}^-}^{(phd)}(\lambda)$  and the inverse "bremsstrahlung" rate coefficient  $K_{ea,ff}(\lambda, T)$  introduced in Eqs. (26) - (28), which cause the efficiencies of these processes, are determined here using the data presented in Stille & Callaway (1970) and Wishart (1979).

According to Eq. (29) the efficiencies of the processes (11) of the considered metal atoms photo-ionization depend on the densities  $N([X]; h)$  of these atoms and on the mean photo-ionization cross-sections  $\sigma_{[X]}^{(phi)}(\lambda; T)$ . These cross-sections for the atoms of all relevant metals ( $\text{Na}$ ,  $\text{Ca}$ ,  $\text{Mg}$ ,  $\text{Si}$ ,  $\text{Al}$ ,  $\text{Fe}$ ) are calculated here in the wide region of  $\lambda$  and  $T$  on the basis of the data from Travis & Matsushima (1968). The densities  $N([X]; h)$  are determined from Saha's equation, with given  $T$ ,  $N(e)$  and the ion densities  $N(X^+)$ . For that purpose is needed to know the corresponding partition functions  $Q_{[X]}(T; \delta_X)$ , where  $\delta_X \equiv \delta I_X(T; N(e))$  is the lowering of the ionization potential of the given ground state atom  $X$ . The calculation of the partition functions, which is the key element of the whole procedure of  $N([X]; h)$  determination, is performed here on the basis of the data from Drawin & Felenbok (1965).

However, because of this source of the data about the partition functions it is needed to stay for a moment on this point. The reason for this is the fact that the partition functions are calculated in Drawin & Felenbok (1965) for the values of  $\delta I_X$  from the region which is limited from below with 0.1 eV, while in our case ( $N(e) \cong 10^{12} \text{cm}^{-3}$ ,  $T \cong 3500 \text{K}$ ) we have that  $\delta I_X \sim 10^{-4} \text{eV}$ . As it is known in the Saha's equation  $\delta I_X$  appears also in the argument of its ex-

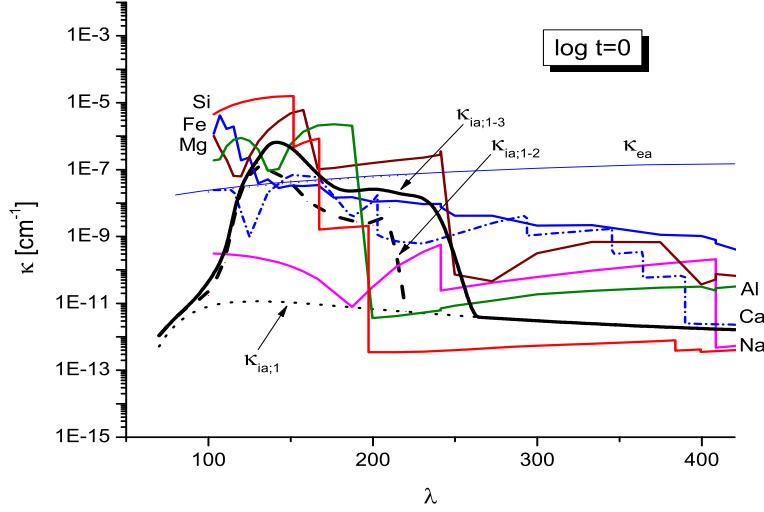


**Figure 3.** The plots of all considered absorption processes for  $\log \tau = 0$  in the case of the sunspot (umbral model M from Maltby et al. (1986)): Mg, Si, etc. - the abbreviations for the spectral coefficients  $\kappa_{phi;X}$  of the metal atoms photo-ionization processes (11) with  $X = \text{Mg, Si, etc.}$ ;  $\kappa_{ea}$  - the electron atom processes (9) and (10) together ( $\text{H}^-$ -continuum);  $\kappa_{ia;1}$  - symmetric ion-atom processes (1) and (2) together ( $\text{H}_2^+$ -continuum);  $\kappa_{ia;1-2}$  - ion-atom symmetric and non-symmetric processes (3) - (5);  $\kappa_{ia;1-3}$  - all ion-atom processes, including non-symmetric processes (6) - (8).

ponent, but in the considered case  $\delta I_X/kT \lesssim 10^{-3}$  and the influence of  $\delta I_X$  on the values of that exponent can be completely neglected. However, the fact that existing  $\delta I_X \ll 0.1$  eV has to be examined from the aspect of its influence on the partition functions. Namely, the moving of the value of  $\delta I_X$  from 0.1 eV to about  $10^{-4}$  eV causes the increasing of the principal quantum number of the last realized excited atomic state from about 11 to about 200. It was shown that such increasing of the largest principal quantum number causes the increasing of the values of the partition functions only for about 0.5 percentage. This result means that the partition functions calculated by using the data from Drawin & Felenbok (1965), which relate to  $\delta_X = 0.1$  eV, were applicable for determination of the densities  $N([X]; h)$ .

## 5 RESULTS AND DISCUSSION

The sunspot model M from Maltby et al. (1986), as well as its differences with the respect to the quiet Sun referent model, also from Maltby et al. (1986), are illustrated by Fig. 2. So, the part of this figure ("a") presents the densities of the hydrogen ions  $\text{H}^+$  and  $\text{H}^-$  and relevant metal ions ( $\text{Na}^+$ ,  $\text{Ca}^+$ , etc.) as the functions of  $h$ . The part ("b") presents the local temperature and the densities of the free electrons and hydrogen atoms ( $T$ ,  $N_e$  and  $N(\text{H})$ ) from the model M together with the corresponding quantities ( $T_{ref}$ ,  $N_{e;ref}$ ,  $N_{ref}(\text{H})$ ) from the referent model, also as the functions of  $h$ .

In accordance with the mentioned in the Introduction we should obtain firstly the picture which reflects the relative efficiencies within the sunspot of all symmetric and non-symmetric ion-atom processes (1) - (2), (3) - (5) and

(6) - (8), as well as the electron-atom absorption processes (9) - (10) and metal atom photo-ionization processes (11). For that purpose the several plots of spectral absorption coefficients of all these processes were performed for the values of  $\log \tau$  between 1.0 and  $-1.0$  in the region  $70 \text{ nm} \leq \lambda \leq 800 \text{ nm}$ . We mean on the ion-atom coefficients  $\kappa_{ia;1}(\lambda; h)$ ,  $\kappa_{ia;1-2}(\lambda; h)$  and  $\kappa_{ia;1-3}(\lambda; h)$ , which are given by Eqs. (19) - (24), as well as on the electron-atom and photo-ionization coefficients, namely  $\kappa_{ea}(\lambda; h)$  and  $\kappa_{phi;[X]}(\lambda; h)$ , which are given by (27) and (29) respectively. It was established that in the short wave part of this spectral region, generally we have the domination of the photo-ionization processes (11) in respect to all other considered absorption processes. So, for  $-1.0 \leq \log \tau \leq 0.5$  the mentioned domination exists in the region  $\lambda \lesssim 250 \text{ nm}$ , but with the increasing of the value of  $\log \tau$  this region decreases and for  $\log \tau = 1.0$  the region of this domination is  $\lambda \lesssim 175 \text{ nm}$ .

In the same time it was established that the electron-atom absorption processes (9) - (10) can be treated now as the referent processes not only in the case of the quiet Sun photosphere, but also in the case of a sunspot. Moreover, for any value of  $\log \tau$  just these processes dominate in the best part of the whole considered spectral region in respect to all other absorption processes, including the processes (11). All mentioned is illustrated by Fig's. 3 and 4 which show the plots of all considered absorption processes for  $\log \tau = 0.5$  and  $0.0$  respectively. Let us note that the plots for  $\log \tau = 0.5$  were needed since just in the region  $\log \tau > 0.0$  the density of the  $\text{H}^+$  ions becomes very fast increasing.

In Fig's. 3 and 4 the plot of each of all considered photo-ionization processes (11) is shown separately. These plots are marked by designations of the corresponding atoms ("Mg", "Si", etc.). We draw attention that here was not planed to

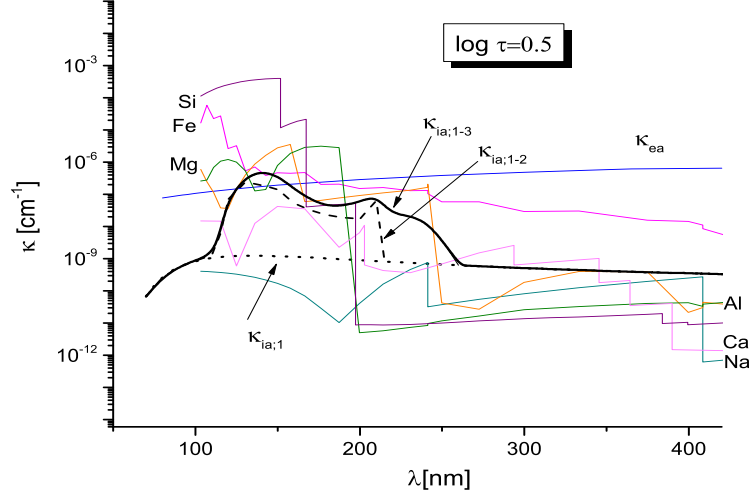


Figure 4. Same as in the Fig. 4 but for  $\log \tau = 0.5$

obtain the plot describing the total efficiency of all photo-ionization processes. Namely to obtain such a plot would be certainly useful in the context of the synthesis of the corresponding sunspot spectrum. However, such task is out of the frame of the present work.

The electron-atom processes (9) - (10), which are treated sometimes as the  $H^-$ -continuum, are represented here by their common plot which in these figures is marked by  $\kappa_{ea}$ . However, in accordance with the aims of this work, the examined ion-atom absorption processes are characterized by three corresponding plots, namely: one for the whole group "1", i.e. the symmetric processes (1) and (2), which are known also as the  $H_2^+$ -continuum; second for these first processes together with the non-symmetric processes of the group "3", i.e. (3) - (5); third for all considered ion-atom processes together, including the non-symmetric processes of the group "3", i.e. (1) - (2). These plots are marked here by " $\kappa_{ia;1}$ ", " $\kappa_{ia;1-2}$ " and " $\kappa_{ia;1-3}$ " respectively. The presented ion-atom plots show that it was indeed necessary to take into account additional non-symmetric processes of the group "3". Namely, one can see that the inclusion of these processes significantly increases the total efficiency of the non-symmetric ion-atom absorption processes.

The figures 3 and 4 demonstrate that the total efficiencies of all considered symmetric and non-symmetric ion-atom absorption processes in the region  $110 \text{ nm} \lesssim \lambda \lesssim 230 \text{ nm}$  is of the same order of the magnitude as the one of the electron-atom processes (9) - (10) together ( $H^-$ -continuum). However, here is needed to emphasis that in the significant part of this region these total efficiencies are close, or the ion-atom efficiency is even larger than electron-atom one.

From Fig. 2 one can see that the plasma temperature in sunspot ( $T$ ) is significantly smaller than in the case of the quiet Sun ( $T_{ref}$ ) in the larger part of that region of  $\log \tau$  or  $h$  which is shown in this figure. Consequently, it was possible to expect that in this region the relative importance of the non-symmetric absorption processes (in respect to the

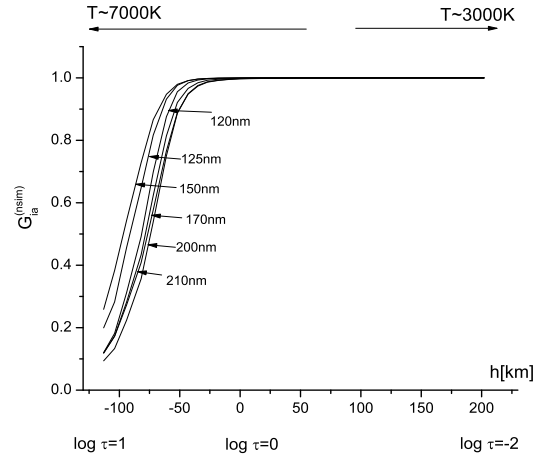
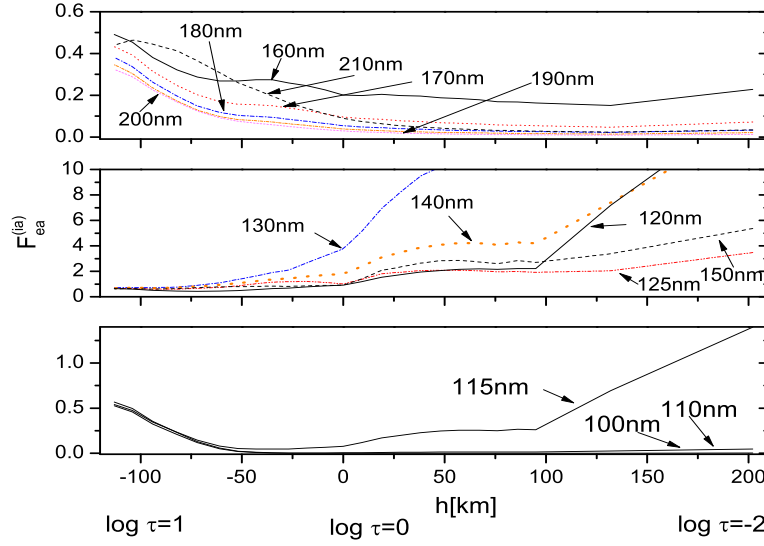


Figure 5. The behavior of the quantity  $G_{ia}^{(nsim)}(\lambda; h)$ , given by equation (30), which characterizes the relative efficiency of all non-symmetric ion-atom processes in respect to the total efficiency of all ion-atom absorption processes (the sunspot model M from Maltby et al. (1986)).

symmetric ones), at least for  $110 \text{ nm} \lesssim \lambda \lesssim 230 \text{ nm}$ , will be larger than in the case of the quiet Sun. In order to test this assumption and to establish what is the contribution of all considered non-symmetric processes to the total ion-atom efficiencies in far UV region of  $\lambda$  we have determined the adequately defined quantity  $G_{ia}^{(nsim)}(\lambda; h)$ , namely

$$G_{ia}^{(nsim)}(\lambda; h) = \frac{\kappa_{ia;2}(\lambda; h) + \kappa_{ia;3}(\lambda; h)}{\kappa_{ia;1-3}(\lambda; h)}, \quad (30)$$

where  $\kappa_{ia;j}(\lambda)$ , with  $j = 2$  and  $3$ , and  $\kappa_{ia}(\lambda; h)$  are given by Eqs. 22 and 24 respectively. The behavior of this quantity (for several values of  $\lambda$ ) is illustrated by Fig. 5 in the interval of heights:  $-125 \text{ km} \leq h \leq 200 \text{ km}$ . From this figure one can see that in far UV region the non-symmetric processes are



**Figure 6.** The behavior of the quantity  $F_{ea}^{(ia)}(\lambda; h)$ , given by equation (31), which characterizes the relative efficiency of all (symmetric and non-symmetric) ion-atom processes with respect to the total efficiency of the electron-atom absorption processes (9) - (10) within the sunspot model M from Maltby et al. (1986).

dominant in respect to the symmetric ones for  $h > 50$  km, i.e. in the largest part of the region of  $h$  shown in Fig. 2, but for  $-75 \text{ km} \leq h \lesssim 50 \text{ km}$  the efficiencies of the symmetric and non-symmetric processes are close. This fact shows that in the case of the sunspot (as in the case of the quiet Sun) it is useful to treat the symmetric and all non-symmetric ion-atom absorption processes together. Finally, we will have to compare within the same part of the sunspot (which is shown in Fig. 2) the total efficiencies of the ion-atom and referent electron-atom absorption processes (9) and (10) together ( $H^-$ -continuum) in the considered part of the far UV region of  $\lambda$ . Already this figure gives the possibility to expect that in the sunspot case these total efficiencies could be close at least in a part of the mentioned spectral region. It can be tested on the basis of the behavior of the quantity  $F_{ea}^{(ia)}(\lambda; h)$ , defined by

$$F_{ea}^{(ia)}(\lambda) = \frac{\kappa_{ia;1-3}(\lambda; h)}{\kappa_{ea}(\lambda; h)}, \quad (31)$$

where  $\kappa_{ea}(\lambda; h)$  is given by Eq. 27. The behavior of this quantity (also for several values of  $\lambda$  from the far UV region) is illustrated by Fig. 6 in the same interval of heights:  $-125 \text{ km} \leq h \leq 200 \text{ km}$ . This figure shows that: for any of the taken  $\lambda$  the total efficiency of all ion-atom absorption processes is close, or even larger than the efficiency of the referent electron-atom processes ( $H^-$ -continuum) in the largest part of the mentioned interval of  $h$ . This means that in the case of the sunspot it is needed to consider the discussed ion-atom absorption process in the mentioned part of the far UV region ( $110 \text{ nm} \lesssim \lambda \lesssim 230 \text{ nm}$ ) always together with the referent electron-atom processes ( $H^-$ -continuum). Consequently, the considered ion-atom processes should be also included *ab initio* in the corresponding models of sunspots of solar-type and near solar-type stars. Due to possible future investigations of these ion-atom processes, the needed

spectral rate coefficients are determined and presented in Appendix B. Since the ion-atom processes of the type (3) - (5) with  $X = \text{Li}$  could be interesting in connection with the so called lithium stars (mentioned in the Introduction), the corresponding spectral rate coefficients are also presented in this Appendix.

## 6 CONCLUSIONS

From the presented material it follows that the considered symmetric and non-symmetric ion-atom absorption processes influence on the opacity of sunspots in the considered spectral region ( $110 \text{ nm} \lesssim \lambda \lesssim 230 \text{ nm}$ ) not less and in some parts even larger than the referent electron-atom processes. The presented results show that further investigations of the non-symmetric ion-atom absorption processes promise that their efficiency could be increased considerably. Namely, the processes (3) - (5) with  $X = \text{Fe}$  were not considered here because of the absence of the data about the needed characteristics of the corresponding molecular ion. However the Fe component, according to Fig. 2, gives the significant contribution to the electron density. Also, some of the possible processes of the (satellite) type (6) - (8) could be very efficient. It means that the inclusion in the consideration of all possible relevant non-symmetric ion-atom absorption processes would surely increase their total efficiency. Because of that, we take such inclusion as the task for the investigations in the nearest future. For this purpose, here are presented the spectral characteristics of the considered ion-atom absorption processes which can be used in some further applications.

Finally, the presented results show that in far UV region the significance of the considered ion-atom absorption processes is sufficiently large that they should be included



*ab initio* in the corresponding models of the sunspots. Apart of that, obtained results could be useful also in the case of different solar like atmospheres.

## ACKNOWLEDGMENTS

The authors wish to thank to Profs. V.N. Obridko, A.A. Nusinov and N. S. Polosukhina for the shown attention to this work. Also, the authors are thankful to the Ministry of Education, Science and Technological Development of the Republic of Serbia for the support of this work within the projects 176002, III4402.

## REFERENCES

- Aymar, M., & Dulieu, O. 2012, *Journal of Physics B Atomic Molecular Physics*, 45, 215103
- Drawin, H.-W., & Felenbok, P. 1965, *Data for plasmas in local thermodynamic equilibrium*, by Drawin, Hans-Werner.; Felenbok, Paul. Paris, Gauthier-Villars, 1965.
- Fontenla, J. M., Avrett, E., Thuillier, G., & Harder, J. 2006, *ApJ*, 639, 441
- Fontenla, J. M., Curdt, W., Haberleiter, M., Harder, J., & Tian, H. 2009, *ApJ*, 707, 482
- Fontenla, J. M., Harder, J., Livingston, W., Snow, M., & Woods, T. 2011, *Journal of Geophysical Research (Atmospheres)*, 116, 20108
- Habli, H., Ghalla, H., Oujia, B., & Gadéa, F. X. 2011, *European Physical Journal D*, 64, 5
- Hack, M., Polosukhina, N. S., Malanushenko, V. P., & Castelli, F. 1997, *A&A*, 319, 637
- Heine V. 1970, *Solid State Physics* 24, 1-36.
- Ignjatović, L. M., & Mihajlov, A. A. 2005, *Phys.Rev.A*, 72, 022715
- Ignjatović, L. M., Mihajlov, A. A., & Klyucharev, A. N. 2008, *Journal of Physics B Atomic Molecular Physics*, 41, 025203
- Ignjatović, L. M., Mihajlov, A. A., Sakan, N. M., Dimitrijević, M. S., & Metropoulos, A. 2009, *MNRAS*, 396, 2201
- Ignjatović, L. M., Mihajlov, A. A., Srećković, V. A., & Dimitrijević, M. S. 2014, *MNRAS*, 439 (3), 2342
- Maltby, P., Avrett, E. H., Carlsson, M., Kjeldseth-Moe, O., Kurucz, R. L., Loeser, R. 1986, *ApJ*, 306, 284
- Mihajlov, A. A., & Dimitrijević, M. S. 1986, *A&A*, 155, 319
- Mihajlov, A. A., Dimitrijević, M. S., & Ignjatović, L. M. 1993, *A&A*, 276, 187
- Mihajlov, A. A., Dimitrijević, M. S., Ignjatović, L. M., & Djurić, Z. 1994, *A&AS*, 103, 57
- Mihajlov, A. A., & Ignjatović, L. M. 1996, *DIAM Dynamique des Ions, des Atomes et des Molecules, Contrib. Papers*, p. 157
- Mihajlov, A. A., Ignjatović, L. M., Sakan, N. M., & Dimitrijević, M. S. 2007, *A&A*, 437, 1023
- Mihajlov, A. A., Ignjatović, L. M., Srećković, V. A., Dimitrijević, M. S. & Metropoulos, A. 2013, *MNRAS*, 431, 589
- Nguyen, J. H. V., Viteri, C. R., Hohenstein, E. G., Sherill, C. D., Brown, K. P., & Odom, B. 2011, *New Journal of Physics*, 13, 063023

- Penn, M. J., & Livingston, W. 2011, *IAU Symposium*, 273, 126
- Shavrina, A. V., Polosukhina, N. S., Zverko, J., et al. 2001, *A&A*, 372, 571
- Shavrina, A. V., Polosukhina, N. S., Pavlenko, Y. V., et al. 2003, *A&A*, 409, 707
- Skenderović, H., Beuc, R., Ban, T., & Pichler, G. 2002, *European Physical Journal D*, 19, 49
- Srećković, V. A., Mihajlov, A. A., Ignjatović, L. M. & Dimitrijević, M. S. 2013, *Adv. Space. Res.*, doi:10.1016/j.asr.2013.11.017.
- Stancil, P. C., Kirby, K., Sannigrahi, A. B., Buenker, R. J., Hirsch, G., Gu, J.-P. 1997, *ApJ*, 486, 574
- Stilley, J. L., & Callaway, J. 1970, *ApJ*, 160, 245
- Travis, L. D., & Matsushima, S. 1968, *ApJ*, 154, 689
- Vernazza, J., Avrett, E., & Loser, R. 1981, *ApJS*, 45, 635
- Veža, D., Beuc, R., Milošević, S., & Pichler, G. 1998, *European Physical Journal D*, 2, 45
- Wishart, A. W. 1979, *MNRAS*, 187, 59

## APPENDIX A: THE MOLECULAR ION CHARACTERISTICS

The potential curves of the ground and several low lying excited electronic states of the molecular ions  $\text{HNa}^+$  and  $\text{HLi}^+$ , as well as the corresponding transition dipole matrix elements, are calculated here by means of the method which was described in details in Ignjatović & Mihajlov (2005). The calculated characteristics of these molecular ions are shown as the functions of the internuclear distance  $R$  in Fig's. A1 and A2, where the zero of the energy is chosen in such a way that the potential energy  $U_1(R)$  of the ground electronic state is equal to zero at  $R = \infty$ . In these figures are given the characteristics not only of the ground and first excited electronic state with the energy  $U_2(R)$ , but also of the several excited states whose energies are larger then  $U_2(R)$ . Namely, we keep in mind that such excited electronic state of the ions  $\text{HNa}^+$  and  $\text{HLi}^+$  could be needed in some further applications.

The mentioned calculation method was developed for the molecular ions  $A_2^+$ ,  $AB^+$  and  $HB_2^+$ , where  $A$  and  $B$  are the alkali metal atoms (Li, Na, etc.). Within this method the wave functions of the adiabatic electronic states of the considered molecular ion are described in the single-electron approximation, under the condition which are analogous to the orthogonality conditions in the known pseudopotential method of Heine (1970). Using this method, in Ignjatović & Mihajlov (2005) were successfully determined the potential curves and the dipole matrix elements of the ions  $\text{Na}_2^+$  and  $\text{Li}_2^+$ , and later in Ignjatović et al. (2008) - of the ion  $\text{LiNa}^+$ . Let us note that the first version of this method was used in Mihajlov & Ignjatović (1996) just in the connection with the radiative processes in  $(\text{H} + \text{Li}^+)$ -collisions.

## APPENDIX B: THE BEHAVIOR OF THE SPECTRAL CHARACTERISTICS

The spectral rate coefficients  $K_{X;2}(\lambda; T)$  and  $K_{X;3}(\lambda; T)$  for the non-symmetric processes (3) - (5) and (6) - (8) respec-

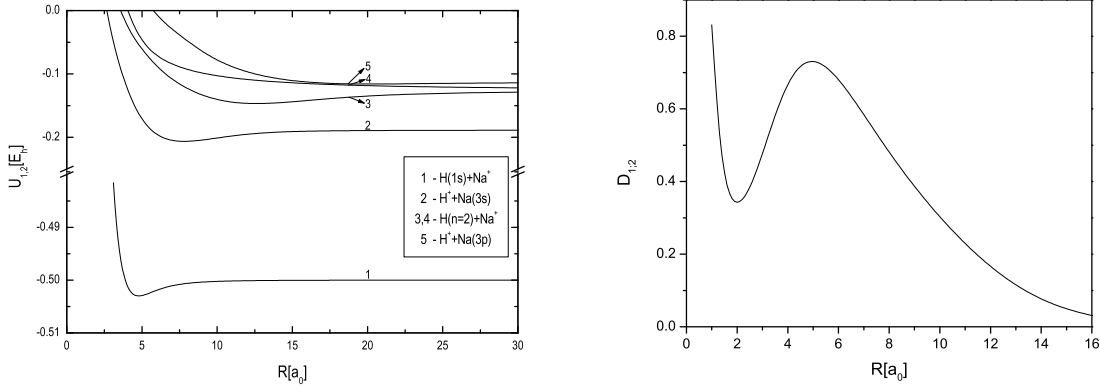


**Figure A1.** *Left panel a:* The potential curves of the several low lying electronic states of the molecular ion  $\text{HNa}^+$ . *Right panel b:* The matrix elements of the transition dipole moment for the given electronic states of the molecular ion  $\text{HNa}^+$ .

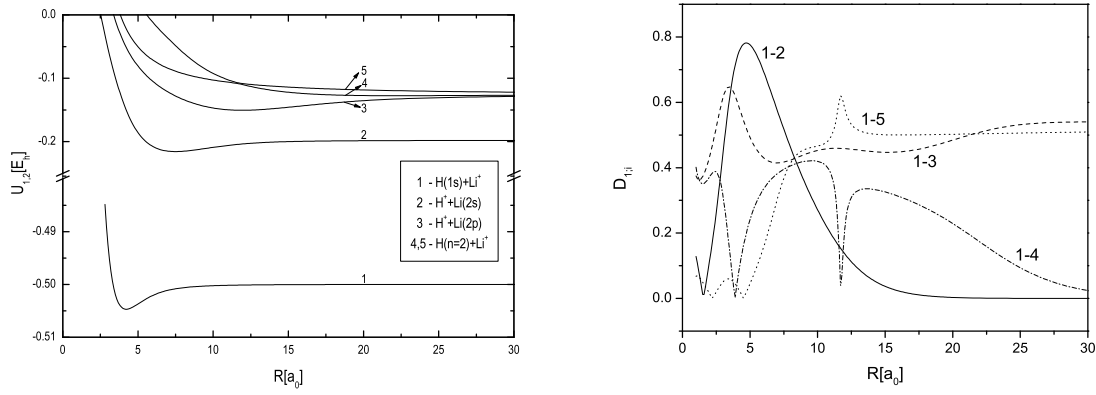


**Figure A2.** *Left panel a:* Same as in Fig. A1 side a, but for the molecular ion  $\text{HLi}^+$ . *Right panel b:* Same as in Fig A1 side b, but for the molecular ion  $\text{HLi}^+$ .

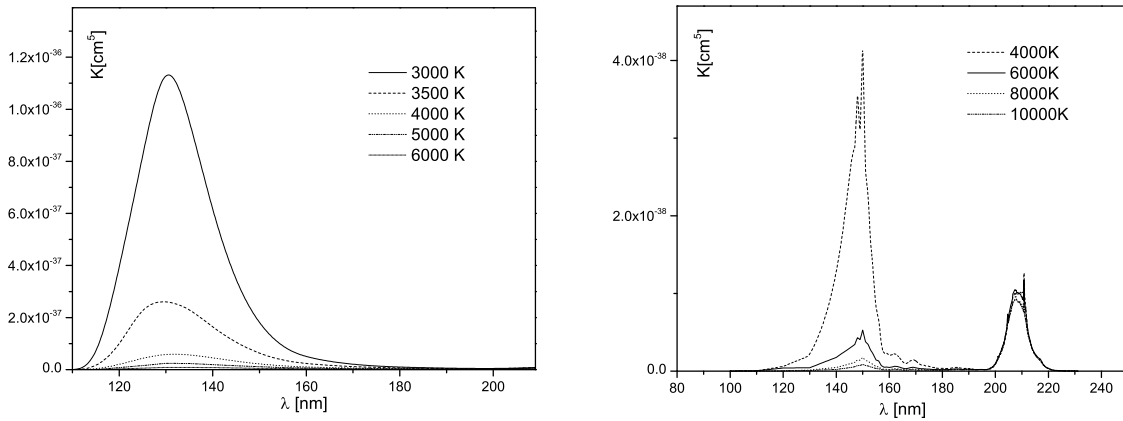


**Figure B1.** *Left panel a:* The behavior of the spectral rate coefficients  $K_{X;j=2}(\lambda, T)$ , given by Eq. (21), which characterize all non-symmetric ion-atom absorption processes (3)-(4) with  $X=\text{Mg}$ . *Right panel b:* Same as in left panel, but for  $X=\text{Si}$ .

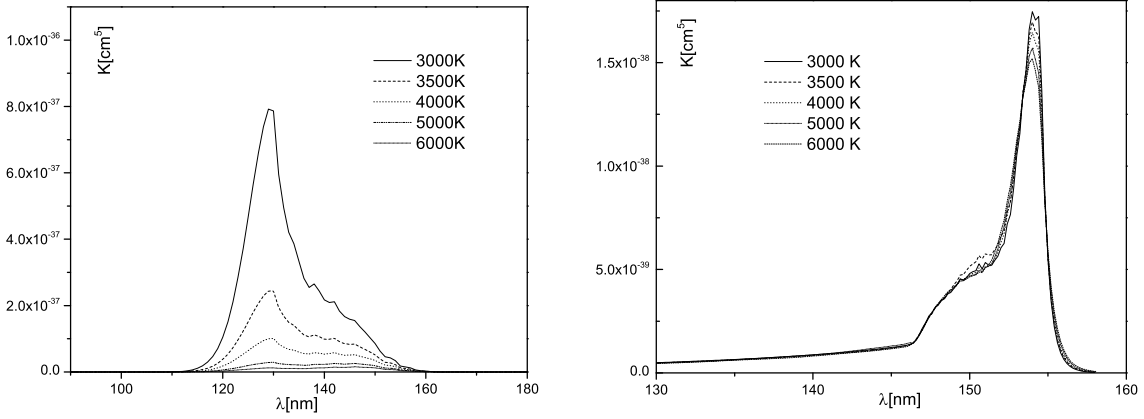


**Figure B2.** *Left panel a:* Same as in Fig. B1, but for  $X=\text{Ca}$ . *Right panel b:* Same as in Fig. B1, but for  $X=\text{Na}$ .

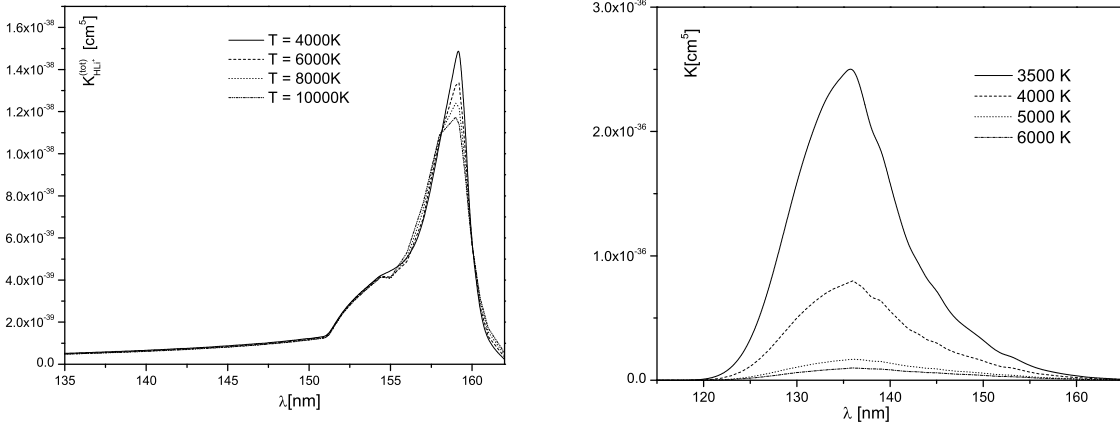


**Figure B3.** *Left panel a:* Same as in Fig B1 but for  $X=\text{Li}$ . *Right panel b:* The behavior of the spectral rate coefficients  $K_{X;j=3}(\lambda, T)$ , given by Eq. (21), which characterize satellite ion-atom non-symmetric absorption processes (6)-(7) with  $X^{++}=\text{Ca}^{++}$ .

tively, which can be used in some further applications, are presented here in the relevant regions of  $\lambda$  and  $T$ . Since the properties of the behavior of the similar spectral rate coefficients were already discussed (with quite a lot of details) in Mihajlov et al. (2013), here they are shown in Fig's. B1 - B3 without additional comments.